Colloid Polym Sci 276:1024–1031 (1998)

ORIGINAL CONTRIBUTION

W.-M. Kulicke
O. Arendt
M. Berger

Characterization of hydroxypropylmethylcellulose-stabilized emulsions

Part II: The flow behaviour

Received: 12 May 1998
Accepted: 24 June 1998

W.-M. Kulicke (✉) · O. Arendt · M. Berger
Institute of Technical
and Macromolecular Chemistry
University of Hamburg
Bundesstr. 45
D-20146 Hamburg
Germany

Abstract Emulsions stabilized with hydroxypropylmethylcellulose were characterized with respect to their particle size and their flow behavior. This part of the study focuses on the latter.

During shear experiments an increase in viscosity was detected with increasing phase volume fraction. After a critical phase volume fraction, ϕ, of 0.6 had been exceeded, yield stresses of between 7 and 17 Pa were exhibited. In the emulsions without yield stress the relative emulsion viscosities were examined against the relevant theories, which resulted in good agreement being found with the predictions of Krieger and Dougherty. Using the extrapolated maximum phase volume fraction, it was thus possible to calculate the thickness of the adsorbate layer as approximately 60 nm.

In the dynamic measurements, a maximum was determined for the material functions. This was attributed to shear-induced restructuring processes in the emulsions. The dynamic measurements in the linear viscoelastic range showed that, in spite of increasing phase volume fraction, the critical relaxation time decreased, whereas the values of the moduli rose at small oscillation frequencies.

Time-dependent measurements showed that thixotropy was detected for emulsions with a phase volume fraction of $\phi \geq 0.7$.

Creep tests showed that the compliance fell with increasing phase volume fraction. The zero shear modulus and the relative elastic compliance were calculated for the emulsions that exhibited yield stresses. Good agreement was found between the zero shear modulus and the values for the storage modulus determined in dynamic measurements.

Key words Hydroxypropylmethylcellulose – emulsions – stabilization – flow behavior – rheometry

Introduction

In former investigations, Kulicke et al. have characterized the flow behavior of polysaccharides intensively [1–3 and references cited therein]. In this contribution, emulsions stabilized with hydroxypropylmethylcellulose were characterized in respect to their particle size and their flow behavior. This part of the study focuses on the latter.

The results of the determination of particle size by active laser scanning as well as a detailed introduction are given in part I of this contribution.

Experimental

Preparation of emulsions

See part I.

Rheometry

The rheological measurements were performed with a UDS 200 rheometer from Physica Meßtechnik GmbH (Stuttgart, Germany) with a plate–plate geometry ($d = 5$ cm) at 298 K and a 15 min delay before starting the measurements.

Results and discussion

This part of the paper focuses on shear and dynamic measurements of the emulsions stabilized with hydroxypropylmethylcellulose. Figure 1 shows their viscosity curves.

As the phase volume fraction, ϕ, increases – i.e. with increasing proportion of oil phase – there is a rise in viscosity. However, as ϕ increases, the almost Newtonian flow of the emulsifier solution changes to pseudoplastic flow with shear-thinning of the emulsions.

At a phase volume fraction of $\phi > 0.5$ and shear rates of $\dot{\gamma} < 1\,\mathrm{s}^{-1}$, non-Newtonian flow was observed, which changed to a plateau as the shear rate rose and then also exhibited shear-thinning. If the phase volume fraction exceeded a value of $\phi = 0.6$, yield stresses occurred, which cannot be shown in this figure but are discussed in Fig. 4.

Fig. 1 Viscosity of the emulsions investigated as a function of shear rate

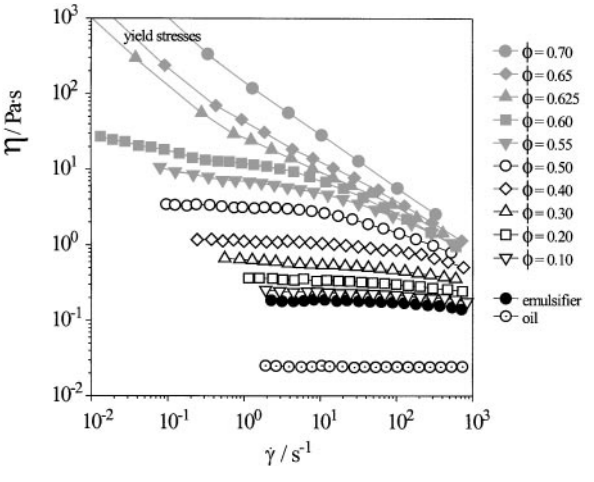

It is noticeable that all the viscosity curves converge in a region of identical gradient. It may therefore be assumed that in this range of higher shear rates a complete breakdown of the extended superstructures has occurred, and that all the particles are spaced equidistantly [4]. These emulsions thus also comply with the constraint that forbids the material functions within a homologous series from crossing over, and at high shear rates the same solution structures are also present.

Furthermore, there was no visual evidence of the emulsion breaking down during the shear measurement, so it may be assumed that no shear-induced destabilization processes were taking place. The shape of the viscosity curves also shows that no dilatant flow was observed in any of the emulsions, as has sometimes been reported for emulsions with very high phase volume fractions and highly viscous inner phases [5].

To account for the increasing viscosity yield as the phase volume fraction, ϕ, rises, two different approaches to describing the particles have been adopted: deformable particles or hard spheres. In deformable particles the viscosity of the dispersed phase has a large influence since an external tension results in transport currents within the particles, and as a result the overall viscosity is lowered. However, this approach only applies when no emulsifiers or stabilizing polymers have been used [6].

If emulsifiers or polymers that form a phase boundary film are used in the emulsion, the particles tend to behave as hard spheres, which is why the term "droplets" is often used when describing the disperse phase of an emulsion. Assuming hard spheres, the easiest case to deal with theoretically is then taken, i.e. that of narrowly distributed, hard, uncharged spheres in a highly diluted solution, so that no interaction can occur between them.

Einstein was able to derive the relative increase in viscosity of the entire solution as a function of the phase volume fraction, ϕ, for this type of suspension [7]. If the outer phase has Newtonian viscosity, then Eq. (1) applies

$$\eta_{\mathrm{rel}} = 1 + 2.5\,\phi \ . \qquad (1)$$

However, Eq. (1) only applies to very low-phase volume fractions of $\phi < 0.05$. In order to describe the rise in viscosity over wider ranges of the phase volume fraction, semi-empirical exponential equations were developed. Thus, a crowding factor, β, was introduced, which – as the reciprocal of the maximum phase volume fraction, ϕ_{m} – assumes a value of 1.35 ($\phi_{\mathrm{m}} = 0.74$) for the most densely packed spheres and a value of 1.91 ($\phi_{\mathrm{m}} = 0.52$) for loosely packed monodisperse spheres with no interaction. A similar type of exponential equation is known under the name Mooney equation [8–10], which changes to the Einstein

Eq. (1) for $\phi \to 0$.

$$\eta_{rel} = \exp\left[\frac{2.5\phi}{1-\beta\phi}\right] \quad \text{with } \beta = \frac{1}{\phi_m}. \tag{2}$$

In addition to the semi-empirical equations, other theoretical approaches have also been pursued. For instance Krieger and Dougherty [11, 12] succeeded in deriving the hard-sphere model from considerations on the theory of corresponding states. This approach also assumes a suspension of small hard spheres, i.e. the layer of adsorbed emulsifier is very much thinner than the radius of the particles. In contrast to the previously presented descriptions, this derivation presupposes that the particles are present in a non-Newtonian medium, e.g. in polymer solutions.

$$\eta_{rel} = \left[1 - \frac{\phi}{\phi_m}\right]^{-[\eta]\phi_m}. \tag{3}$$

This microstructure–viscosity Eq. (3) expresses the relative viscosity, η_{rel}, as a function of the volume fraction, ϕ, of the disperse phase, the intrinsic viscosity, $[\eta]$, of the particles and the maximum phase volume fraction, ϕ_m, at the highest packing density.

However, emulsions are not always necessarily stable to dilution, i.e. during dilution – in contrast to suspensions – changes in the particle size and the distribution of the particle size cannot be ruled out. Consequently, the intrinsic viscosity, $[\eta]$, of emulsion particles cannot be easily determined. Therefore, Eq. (3) for determining the ϕ_m value, in which the viscosity behavior is not merely governed by the space requirement of the disperse phase, is simplified to Eq. (4), with the theoretical value of 2.5 for the intrinsic viscosity of hard spheres having a density of one [13].

$$\eta_{rel} = \eta_k \left[1 - \frac{\phi}{\phi_m}\right]^{-2}. \tag{4}$$

In this form the viscosity, η, of the emulsion is then only expressed as a function of the viscosity, η_k, of the external continuous phase and the phase volume fraction, ϕ. If the reciprocal square roots of the emulsion viscosities, η, are plotted against the phase volume fraction, then the readings lie on a straight line when the hard-sphere model is applied. The maximum phase volume fraction, ϕ_m, can then be determined by extrapolating the intersection of the abscissae (Fig. 2).

In Fig. 2 the viscosity values from Fig. 1 are plotted as reciprocal square root values with error margins against the phase volume fraction, ϕ. The error margins indicated result from the fact that at phase volume fractions of $\phi < 0.2$, even the slightest fluctuations in measurement can produce a relatively large ordinate error in this plot.

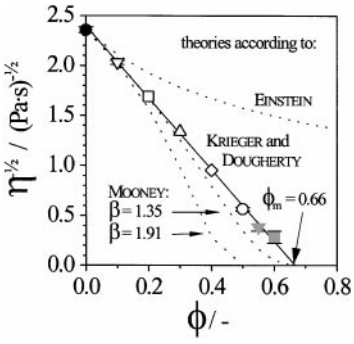

Fig. 2 Viscosity yield of the emulsions as a function of phase volume fraction, ϕ. Solid line: extrapolated according to Krieger and Dougherty, dotted lines: curves according to Einstein and Mooney, respectively

At phase volume fractions of $\phi > 0.5$ it was no longer possible to detect a Newtonian range, so that the plateau value was used for the calculation instead. In addition to the measured values, Fig. 2 also includes for comparison the viscosity values to be expected from the Einstein and Mooney equations, represented by broken lines. The crowding factors, β, used in the Mooney equation thus give corresponding intersections with the abscissae.

At the same time it was observed with this plot that there was a linear relationship for the measured values presented here, thus making linear extrapolation of the readings possible. According to the theory of Krieger and Dougherty the value of the intersection of the abscissae, i.e. for the extrapolation of the viscosity, η, to infinity, yields the maximum phase volume fraction, ϕ_m, as a function of the packing density of the inner phase. For monodisperselely distributed particles that adopt a random packing arrangement, the expected value is $\phi_m = 0.64$, whereas it is $\phi_m = 0.74$ for the densest packing, as already mentioned in Eq. (2).

For the emulsions shown here an extrapolated value of $\phi_m = 0.66$ was determined, which therefore lies only slightly above the expected value of a random packing arrangement. The deviation of 3% might be due to the fact that the theoretical preconditions are not fulfilled in the case of these emulsions; namely of narrowly distributed small particles with no interactions. Furthermore, a yield stress, σ_y, occurs even at $\phi = 0.625$ (cf. Fig. 4), and not simply beyond $\phi > 0.66$, as is otherwise the case. This can be interpreted as an indication of the occurrence of interactions.

With the aid of these data it was possible to show that HPMC is able to form a stable interfacial film, and that the oil particles behave like hard spheres due to the stabilizing adsorbate layer at the phase boundary. If in addition the mean particle radius is known, it is possible with the aid of

Table 1 Yield stresses, σ_y, for emulsions with different phase volume fractions, ϕ

	Phase volume fraction		
	$\phi = 0.625$	$\phi = 0.65$	$\phi = 0.70$
σ_y [Pa]	9.4	16.5	82.3

these data to calculate the thickness of the adsorbate layer [14, 15]. This type of relationship has already been described in a variety of ways and has been confirmed with a wide range of different methods for various emulsion systems, e.g. by means of thin film measurements [16] or low-angle neutron scattering [17].

With the extrapolated maximum phase volume fraction of $\phi_m = 0.66$ and the intrinsic viscosity of hard spheres, $[\eta] = 2.5$, an effective phase volume fraction, ϕ_{eff}, can be calculated that represents the growth in hydrodynamic particle volume by the volume of the adsorbate for each individual particle, by a simple transformation of Eq. (3) to Eq. (5) [14]

$$\phi_{eff} = \phi_m \left[1 - \eta_{rel}^{-[\eta]\cdot\phi_m}\right] . \tag{5}$$

From the calculated effective phase volume fraction, ϕ_{eff}, and that used in the preparation of the emulsions, ϕ, it is possible to calculate the thickness of the adsorbate layer, δ, according to Eq. (6), while taking into account the average particle radius R (cf. Part I, Table 1):

$$\phi_{eff} = \phi\left[1 + \left(\frac{\delta}{R}\right)\right]^3 \Rightarrow \delta = R\left[\left(\frac{\phi_{eff}}{\phi}\right)^{1/3} - 1\right]. \tag{6}$$

Figure 3 shows the phase volume fractions employed, ϕ, (hollow symbols) and the effective phase volume fractions, ϕ_{eff}, (solid symbols) calculated from them.

Fig. 3 Viscosity, η (left-hand y axis, linear scaling), adsorbate thickness, δ, and average particle distance, h_m (right-hand y axis, logarithmic scaling) as functions of the phase volume fraction, ϕ

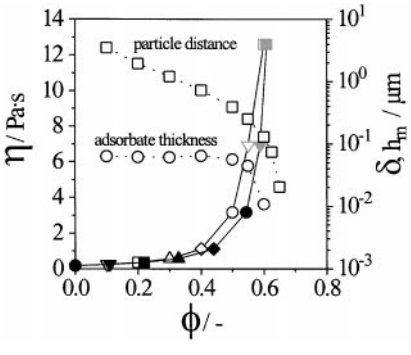

As can be seen from the viscosity data shown, the relative viscosity follows a linear path up to a phase volume fraction of $\phi = 0.4$. In terms of the calculated adsorbate layer this means that it is present in a largely undistributed state, as is confirmed in its horizontal course at approximately 60 nm. Consequently, in this range of low concentration there is still no interpenetration of the particles, i.e. the distance between them is sufficiently large. This suggested that the adsorbed polymer is either stretched or forms multiple layers on the particle surface.

As the phase volume fraction increases, then interpenetration occurs and/or compression of the interfacial film, so that there is a very pronounced reduction of the adsorbate layer. However, since it is impossible to distinguish between these two effects, it must be assumed that both processes occur. If one considers the absolute thickness of the adsorbate layer in the undisturbed system, then it becomes evident that it is considerably thicker than the radius of gyration for the emulsifier would lead one to expect ($\langle R_G^2 \rangle^{1/2} \approx 25$ nm, obtained from SEC/light scattering measurements). It is therefore fair to assume that either several layers of adsorbate, i.e. multiple layers, were present at the phase boundary or that the emulsifier coil had a stretched conformation.

The mean particle distance in the emulsions can also be calculated independently of these considerations. The basis for this calculation is the fact that – as already described – the relative viscosity increases beyond a critical phase volume fraction. If one assumes that the distance between the particles falls below a critical value, then there must be a simple geometric relationship between the mean particle distance, h_m, the particle radius, R, the maximum packing density, ϕ_m, and the phase volume fraction, ϕ. This relationship is established by Eq. (7) [14]

$$h_m = 2\,R\left[\left(\frac{\phi_m}{\phi}\right)^{1/3} - 1\right]. \tag{7}$$

To evaluate Eq. (7), the extrapolated maximum phase volume fraction of $\phi_m = 0.66$ was inserted and the results displayed in Fig. 3 – with reference to the right-hand y-axis. Here it was seen that as the phase volume fraction increased, the particle distance first decreased steadily, before falling sharply at $\phi > 0.4$ and tending towards zero, so that less space is available for the individual particles.

If one considers that these calculations do not take into account any distribution of the particle diameters, but are based upon monodisperse particles with no interactions, then it is surprising how well the individually calculated parameters complement each other and give a unified overall picture.

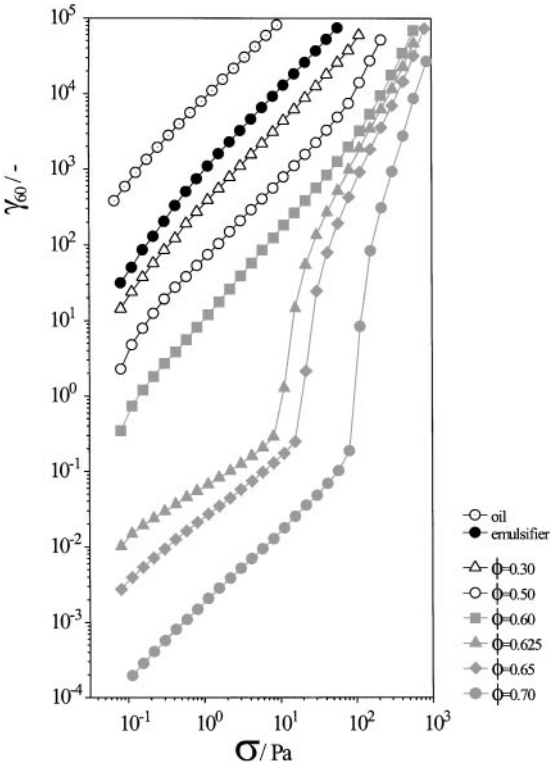

Fig. 4 Determination of yield stresses of the emulsions as functions of the phase volume fraction, ϕ. The curves for the oil phase and for the emulsifying agent HPMC employed (2.5% w/w) are also shown

Yield stresses

The measurements for determining the yield stresses are shown in Fig. 4.

Here the deformation resulting within 60 s, γ_{60}, was plotted against the imposed shear stress. At the beginning a linear relationship was found between deformation and shear stress for both the oil phase and for the emulsifier solution, i.e. Newtonian flow is present.

With $\phi > 0.3$ and $\sigma > 100$ Pa this linear relationship was no longer maintained. Since there was upward deviation of the curves, greater deformation values were obtained, which are equivalent to lower viscosities. This is the region of non-Newtonian flow, shear-thinning now occurred.

At phase volume fractions of $\phi > 0.6$ a completely different curve is seen. These samples did in fact also initially display a linear relationship between shear stress and deformation, but with a significantly smaller gradient. Beyond a certain shear stress there was a sudden, sharp rise in the deformation with only a slight increase in the shear stress. This upward kink in the curve represents the yield stress, since the imposed shear stress is now so great that the inner structure of interactions in the emulsion collapses and a continuous flow is established. When the shear stress was increased still further, a linear relationship was again found, which then changed into a non-linear range of pseudoplastic flow.

Linear regression was carried out in the sections of the curve above and below the kink to evaluate the yield stresses, so that the σ-value at the intercept of the regression lines gave the value of the yield stress, σ_y. The yield stresses thus determined are compiled in Table 1.

A surprising feature is that yield stresses can already be observed even at phase volume fractions significantly smaller than $\phi_m = 0.66$. This and the rise in yield stress with increasing phase volume fraction can be interpreted in several ways. Firstly, the particle size distribution has a decisive influence because small particles are better able to fill the cavities between the larger particles and thus reinforce the structure based on particles. Secondly, and independently of the particle size, partial flocculation of the system makes bond formation between the particles possible, they can then form expansive structures within the emulsion and are thus able to generate a yield stress.

With values between 7 and 17 Pa, the yield stresses in these emulsions are still not sufficiently pronounced for the emulsions to appear rigid, as is the case for example with $\phi = 0.7$. This means that under the influence of gravity these yield stresses are overcome, so that corresponding emulsions, in a beaker for example, can slowly flow together.

Dynamic measurements

Investigations of the viscoelastic properties of substances by means of dynamic measurements can be carried out by two different methods: by determining the linear viscoelastic range at constant oscillation frequency with various amplitudes or with constant amplitude but different frequencies. The advantage of the second method is that if a sufficiently small amplitude is chosen for each frequency, the structure of the solution is not destroyed. The rheometrical parameters obtained are the storage modulus G', as a measure of the elastic flow, and the loss modulus G'', as a measure of the viscous flow, as well as the parameters derived from these.

First the dependence on deformation of these material functions was determined. If changes in the sample can be ruled out, e.g. that may have occurred during filling or in assembling the measuring head, then the substance is in its "rheological base state". The corresponding measurements on the emulsions are shown in Fig. 5.

These amplitude measurements on the emulsions deviate in many respects from those of homogeneous polymer solutions and melts. After the curve has passed through the

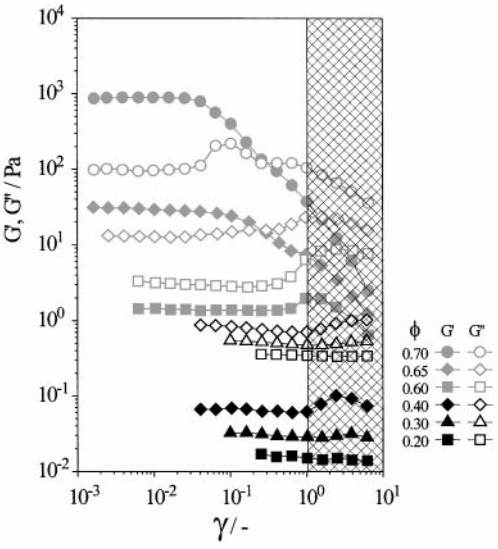

Fig. 5 Deformation measurements of the emulsions: deformations $\gamma > 1$ cause a shear-overlapped dynamic measurement; $\omega = 1$ rad s^{-1}. Solid symbols: storage modulus, G'; hollow symbols: loss modulus, G''

linear viscoelastic range, which was determined for all the emulsions, in some cases an unexpected pattern is observed for the material functions. In the following interpretation it is necessary to take into account the fact that for deformations of $\gamma > 1$ a shear is superimposed upon the oscillation.

In the emulsions with low phase volume fractions, $\phi < 0.4$, practically no deviation from the linear viscoelastic behavior was observed over the entire deformation range. Then at higher phase volume fractions larger deviations in the form of peaks were initially determined for the storage modulus, G', at deformations of $\gamma \geq 1$. As the phase volume fraction increases further, this effect becomes less pronounced, whereas the loss modulus, G'', displays a maximum that is dependent upon the deformation. This is especially clear to see in the emulsion with $\phi = 0.7$.

Since at lower-phase volume fractions the storage modulus initially displayed a maximum, it may be assumed that internal structural changes of the particle arrangement within the emulsions are responsible. Due to the superimposed shear component the particles, which are lying closer to each other, if the phase volume fraction is sufficiently large, are displayed towards each other. Their interaction means that more energy can be stored in the system and so G' increases until this effect has been overcompensated for.

At higher phase volume fractions the particles are more densely packed and at rest tend to form a structure that is then destroyed by the superimposed shear, so that a maximum is determined for G'' which is dependent upon the deformation. At a phase volume fraction of $\phi = 0.7$, and hence with very closely packed particles, the maximum for G'' as previously described, occurred at significantly lower deformations.

One possible explanation for this behavior could be that at large deformations the irregularly oriented particles transform to a more regular state or vice versa. However, another possibility is that the aggregates of particles are destroyed by shear or are restructured. Even shear-induced deformation of the particles must also be regarded as a possible explanation.

For $\phi = 0.4$, the loss factor $\tan\delta (= G''/G')$ is nearly constant in the linear-viscoelastic region, and mainly viscous flow is detected. In the range from $0.4 < \phi < 0.6$ the elastic components increase since now the particles become more closely packed and the steric repulsion of the particles becomes stronger. Beyond the critical phase volume fraction of $\phi_{cr} \geq 0.61$, the storage modulus is dominant over the loss modulus, and the steric interactions between the particles determine the solution structure. At the same time the onset of yield stress is detected (cf. Fig. 5).

Figure 6 is a plot of the storage modulus, G', and loss modulus, G'', as functions of the angular frequency, ω, for various emulsions.

For the emulsions with $\phi = 0.1$ at lower frequencies the storage modulus, G', lay below the loss modulus, G'', since more oscillation energy was dissipated than could be stored reversibly. If the whole of the evaluable frequency range is considered, G' rose more rapidly than G'', so that stronger elastic interactions occurred as the frequency increased. At a critical angular frequency of $\omega_c =$

Fig. 6 Dynamic measurements of emulsions. Solid symbols: storage modulus, G'; hollow symbols: loss modulus, G''

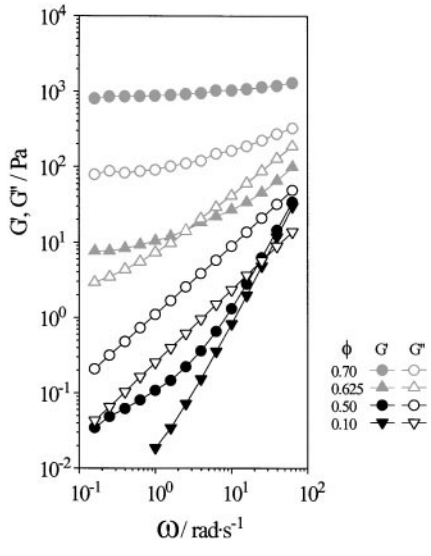

20 rad s^{-1} the material functions cross over and thus characterize the critical relaxation time, $t_c = \omega_c^{-1}$. Above this relaxation time the energy dissipation is negligible, and the system stores the majority of the imposed oscillation energy reversibly. The patterns of these curves represent typical properties of polymer solutions and polymer melts.

At a phase volume fraction of $\phi > 0.4$ a different shape of curve was determined for G' at low frequencies. G' still lies below G'' but as the frequency increases these two material functions first diverge. Consequently, at very small strain frequencies the system is already able to store a significant amount of energy. At these higher phase volume fraction the mean particle distance is so small that the particles and their steric interactions were already able to generate elastic properties by repulsion. Nevertheless, relatively more energy dissipated in this region of the long time scale, e.g. in the diffusion of the particles, than could be stored in the system. The cross-over of the material functions G' and G'' was found at a frequency of $\omega_c = 60$ rad s^{-1}. Although the phase volume fraction was successively increased, the critical relaxation time became shorter contrary to expectations. Hence a different mechanism to that of the particle interaction already described was responsible. It may be assumed that this behavior may be correlated with the polymer solution surrounding the particle. The fewer polymer molecules that were present in these outer phases were less obstructed by entanglements and interactions, as manifested in the shorter relaxation times. For the dynamic measurements presented here, this means that at low frequencies the particulate structure is detected, whereas at higher frequencies the outer phase has a dominant influence on the rheological behavior.

At $\phi = 0.625$ a yield stress then occurred (cf. Fig. 4), and the frequency-dependence plots of G' and G'' exhibited entirely different curves. Elastic properties were now dominant at even the smallest frequencies. This means that the polymer was no longer dominating the flow behavior of the emulsion, but instead strong elastic interactions between the adsorbate layers of the particles in the disperse phase, particularly as the diffusion of the particles was now very severely obstructed. At a frequency of $\omega = 3$ rad s^{-1} an intersection point occurred, above which the emulsion mainly behaved as a fluid, and the viscous properties dominated.

When the phase volume fraction was further increased to a value of $\phi = 0.7$, G' and G'' first showed parallel curves independent of frequency. It was no longer possible to determine an intersection from these parallel curves, meaning that there was an infinitely long relaxation time. As G' was more than a factor of ten greater than G'', the gel state of the emulsion had been reached. G'' rose as the strain frequency increased, as no ideal gel was formed by the particle interactions. In this region the outer phase again determined the flow behavior, so that with the storage modulus, G', practically independent of frequency, the increasing viscous properties again headed towards a point of interaction.

Table 2 Comparison of the storage modulus, G', determined from dynamic measurements at $\omega = 0.1$ rad s^{-1} with the zero shear modulus, G_0, calculated from creep tests for the emulsions that exhibit a yield stress. The relative elastic compliance, J_e/J_{max}, for the corresponding emulsions at a shear stress of $\sigma = 1$ Pa is also included

	Phase volume fraction		
	$\phi = 0.625$	$\phi = 0.65$	$\phi = 0.70$
$G'_{0.1}$ [Pa]	8	31	860
G_0 [Pa]	7	31	837
J_e/J_{max} [%]	22	40	87

In *thixotropic measurements* for the emulsions with a phase volume fraction of $\phi < 0.7$ no structural changes were observed that were dependent upon shear time. This was surprising because yield stresses had already been determined in emulsions with $\phi = 0.625$ and $\phi = 0.65$, which thus had extensive internal structures. In contrast to this thixotropy was detected in an emulsion with $\phi = 0.7$.

Creep tests carried out in the range of viscoelastic deformation with a constant shear stress of 1 Pa showed that the compliance fell with increasing phase volume fraction. When a deformation beyond the linear-viscoelastic range was imposed during the creep tests, no further measurable elastic recovery compliance was detected. The zero shear modulus G_0 and the relative elastic compliance J_e/J_{max} were calculated for the emulsions that exhibited a yield stress (Table 2). Good agreement was found between the zero shear modulus and the values for the storage modulus determined at an angular frequency of $\omega = 0.1$ rad s^{-1}.

Conclusion

In the experiments performed here the thixotropy measurements proved to be very special (measurable effects were only observed for the emulsions with $\phi = 0.7$), and the creep test to be very time-consuming. This would appear to suggest that in the rheometric characterization of emulsions the user is best advised to determine the yield stress, the dynamic properties and one strain sweep.

Acknowledgements We thank "Fonds der Chemischen Industrie" for their support in the form a doctoral grant. In addition we wish to express our most sincere gratitude to the Federal Ministry for Education, Science, Research and Technology and the Deutsche Forschungsgemeinschaft for their financial support.

References

1. Jacobs A, Kulicke W-M (1994) Macromol Symp 84:197
2. Reinhardt UT et al (1994) J Getr Mehl Brot 4:56
3. Kulicke W-M et al (1996) Polymer 37:2723
4. Richardson EG (1953) J Coll Sci 8:367
5. Otsubo Y, Prud'homme RK (1994) Rheol Acta 33:29
6. Taylor GI (1932) Proc R Soc London Ser. A 138:41
7. Einstein A (1906) Ann Phys 19:289; (1911) Ann Phys 24:591
8. Mooney M (1951) J Coll Sci 6:162
9. Dickinson E, Stainsby G (eds) (1982) Colloids in Food 331. Elsevier, New York
10. Pal R (1992) Chem Engng Commun 111:45
11. Krieger IM, Dougherty M (1959) Trans Soc Rheol 3:137
12. Krieger IM (1972) Adv Coll Interf Sci 3:111
13. Kitano T et al (1981) Rheol Acta 20:207
14. Tadros TF (1994) Coll Surf A: Physicochem Eng Asp 91:39
15. Prestidge C, Tadros TF (1988) J Coll Interf Sci 124:660; (1988) Coll Surf 31:325
16. Aston MS et al (1989) Coll Surf 40:49
17. Cairns RH, Ottewill RH (1976) J Coll Interf Sci 54:45